Heat dissipation performance of a high-brightness LED package assembly using high-thermal conductivity filler

K. C. Yung, H. Liem, and H. S. Choy*

Department of Industrial and Systems Engineering, The Hong Kong Polytechnic University, Hung Hom, Kowloon, Hong Kong

*Corresponding author: choy.henry@polyu.edu.hk

Received 9 August 2013; accepted 1 November 2013;
posted 7 November 2013 (Doc. ID 195552); published 4 December 2013

This paper presents a thermal analysis and experimental validation of natural convective heat transfer of a high-brightness light-emitting diode (LED) package assembly. The substrate materials used in the LED package assembly were filled and doped using boron nitride (BN) filler. The thermal conductivity of the BN-filled substrate was measured. The temperature distribution and heat flow of the LED package were assessed by thermal profile measurement using an infrared (IR) camera and thermocouples. In addition, the heat transfer process of the LED package assembly in natural convection was also simulated using the computational fluid dynamics method. The optical performance of the LED package was monitored and investigated with various filler contents. The heat conduction mechanism in the substrate was analyzed. IR thermogram showed that the BN-doped substrate could effectively lower the surface temperature of the LED package by 21.5°C compared with the traditional FR4 substrate. According to the *IESNA LM 80* lifetime testing method, reduction in LED temperature can prolong the LED's lifetime by 19,000 h. The optical performance of the LED package assembly was also found to be improved significantly in lighting power by 10%. As a result, the overall heat dissipation capability of the LED package to the surrounding is enhanced, which improves the LED's efficacy.

OCIS codes: (000.6850) Thermodynamics; (160.5470) Polymers; (110.6820) Thermal imaging.
http://dx.doi.org/10.1364/AO.52.008484

1. Introduction

Over the past few years, high-brightness light-emitting diodes (LEDs) have penetrated into a number of lighting applications, including indoor lighting, street lamps, advertising displays, backlights for LCD TV, traffic lights, and decorative lighting. LEDs that use from 500 mW to as much as 10 W in a single package have become standard and researchers expect that even higher power levels will be used in the future. The luminous efficiency of LEDs has also improved to a certain extent in response to the various applications. At first, gains were made in efficiency so that 20 lm/W had been achieved quickly. Efficiency has slowly risen in the past few years to around 100 lm/W and the trends indicate that 150 lm/W and higher efficiency will occur in the next few years. Even though these high-brightness LEDs have a high energy efficiency of around 15%–25% from power to light versus 10% in traditional lighting, there is still a significant amount of heat being generated. Heat management is thus an important issue for high-brightness LEDs. Narendran and Gu [1] demonstrated experimentally that the life of LEDs decreases in an exponential manner as the junction temperature increases. Therefore, a low operating temperature is essential for LEDs. The use of LED lighting in a given region requires a uniform luminous flux, also known as illuminance [2]. Therefore, it is

1559-128X/13/358484-10$15.00/0

necessary to adopt the form of an LED array and increase its brightness and light-emitting area, to improve the uniformity of illumination.

To overcome the poor heat dissipation problem of a conventional LED package assembly, current trends of encapsulating heat-dissipating electronic components with epoxy resins have stimulated interest in the thermal conductivity of particulate-filled epoxy resins. The low thermal conductivity of epoxy resin can be enhanced by addition of inorganic particles with high thermal conductivity. Electrical insulation is maintained if these particles are electrically insulating [3–6]. Since the thermal conductivity of inorganic filler is much larger than that of the resin matrix, the magnitude of thermal conductivity of the imbedded particles plays a minor role compared with the role of the geometrical arrangement of the particles. Experimental and theoretical investigations [7,8] indicate that the temperature within each particle is approximately uniform, but depends on the location of the particle. It is also found that microsized inorganic filler–epoxy composite usually has much lower breakdown strength [9].

First, the printed circuit board (PCB) material on which the LED package is to be mounted is a concern. Metal-core PCBs (MCPCBs) are normally used as substrates for heat dissipation in LED package units and LED array systems [10,11]. They incorporate a base metal as an integral part of the circuit board, which acts as a heat spreader. The metal core is usually made of an aluminum alloy sandwiched between two dielectric layers for electrical insulation. These dielectric layers become a bottleneck for efficient heat dissipation and can even have thermal conductivity 4–16 times higher than that of traditional FR4 dielectric. FR4 is still used commonly in LED circuit boards due much lower material cost than that of MCPCBs. In addition, it is commercially available and suitable for use with large boards. The base materials of FR4 are typically epoxy and woven fiberglass, which are the worst heat-conducting materials, with thermal conductivity of approximately 0.2–0.3 W/mK [12,13]. The intrinsic limitation of the material thermal properties of traditional FR4 cannot meet the heat dissipation requirements. Pure epoxy substrates are nowadays the alternative materials for LED arrays to be mounted by LED manufacturers as they reduce the product cost, but the thermal conductivity of traditional epoxy resin is much below 0.3 W/mK. For enhancing the thermal conductivity of MCPCBs, FR4 and epoxy substrates, silicon carbide (SiC) [14,15], alumina (Al_2O_3) [15,16], aluminum nitride (AlN) [17–19], and boron nitride (BN) [20] are added to a resin matrix to form a composite having satisfactory properties. The dielectric constants of SiC, Al_2O_3, and AlN are relatively high (>8), which is not satisfactory for electronic encapsulation. BN distinguishes itself by having the lowest dielectric constant, ~4 [21]. In addition, the former three fillers are more expensive than BN and AlN suffers the disadvantage of reactivity with water. BN has a crystal structure similar to that of graphite, with lattice parameters $a = 0.25040$, $b = 0.66612$, and a low dielectric constant $\varepsilon_{\parallel} = \varepsilon_{\perp} = 4$, except where there is a difference in the stacking of the layers [21]. In its powder form, BN is a naturally lubricious material and is often called white graphite. It is also an electrical insulator and exhibits excellent resistance to oxidation, performs exceptionally well at high temperatures (up to 3000°C), and is resistant to corrosion. Its thermal conductivity can reach as high as 60–100 W/mK in powder form. Only BN has been proved to be a good candidate for making filler–epoxy composites, provided the required mixing content is not too high (40%) since it lowers the mechanical strength of the filler–epoxy composite [22]. Also, several different grades of polycarbonate (PC), a type of thermoplastic, have been optimized for use as LED parts, including reflectors, diffusers, and lenses. PC reflectors provide diffuse light from LED-based troffers, while PC-based heat sinks and PC lenses with ultraviolet (UV) protection can offer increased design flexibility to the manufacturers of LED replacement lamps and luminaires. However, its low thermal conductivity of around 0.19–0.2 W/mK affects the overall thermal management of the LED package assembly. Thus, the thermal and optical performance of a LED package assembly with MCPCB, FR4, epoxy, and PC substrates under different thermal conductivity conditions requires further investigation.

The efficiency and reliability of solid-state lighting devices greatly depend on successful thermal management, according to Weng [23]. This plays a key role in controlling the cost effectiveness of LED systems [24–26] in expanding the market. Packaging materials affect the optical efficiency of a LED package significantly. Reflectivity, transmissivity, and index of refraction are all material properties that could affect the lumens output. Thermal issues account for as much as 50% of the failures in lighting. The stability of packaging materials such as encapsulants and lenses is also affected by exposure to elevated temperatures, and UV and radiation of other wavelength.

There is no standard LED package for assessing thermal performance. The substrate material and the environmental condition are critical factors in controlling the thermal dissipation in the package. A study of the heat transfer in a LED package assembly that takes into account the two critical factors is lacking in the literature. In order to overcome the technological gap in the above problem, a thermal and optical study of the LED performance as depicted in Fig. 1(a) is thus proposed. The following work demonstrates the efficacy of the proposed approach for heat dissipation from the LED package assembly using filler material.

2. Experimental Method

High-power white LEDs were used in this study. The total heat generation during the operation of a LED

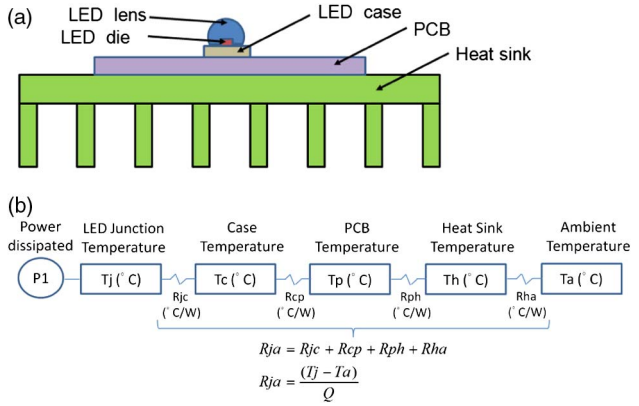

Fig. 1. (a) Schematic diagram of the LED package assembly. (b) LED thermal model diagram.

by a DC power source was determined using the power law equation and the control circuit. The LEDs were connected together in series and a constant current was supplied to each LED using the constant current mode of an Agilent DC power supply. The thermal resistance model calculation using a LED package on a heat sink [27] is shown in Fig. 1(b). Different substrate materials doped with different BN filler contents in weight were prepared and studied. The experimental methods used in this study are described in the following sections.

A. Thermal Imaging

Infrared (IR) thermography (TH9100, NEC-San-ei Co., Japan) was used for assessing the thermal performance of the LED package assembly. In this system, the surface temperatures of the LEDs were determined by IR radiation (of 8–14 μm wavelength) from the surfaces according to Stefan–Boltzmann law. A close-up lens was also fitted to the IR camera (TH91-386, NEC-San-ei Co., Japan). The minimum detection temperature variation is 0.06°C and the minimum spatial resolution is 95 μm × 95 μm. The LEDs were encapsulated in plastic material. The emissivity value was set at 0.95 by referring to the thermal imaging emissivity table. Thermocouples were also used for measurement and calibration, even though the measurement points were limited. Temperatures were recorded after their fluctuation was minimized. The minimization is indicated by the small voltage change across the thermocouple leads. Temperature data were sampled for 10 min at intervals of 1 min and the average was defined as the temperature of each measurement point. To reduce the thermal resistance between the contact interface between the LED and the PCB, silver flake-loaded epoxy was used. The epoxy has a high thermal conductivity of 1.6 W/m°C.

B. Electroluminescence Spectra

Philips Lumileds LEDs were used in this test. They employ a multi-quantum-well structure having layers of InGaN/GaN on a sapphire substrate. The LED die has a standard area of ~1 mm × 1 mm, configured in a wire-bond manner [28], and is encapsulated with an epoxy lens/YAG fluorescent substance/InGaN/GaN chip structure. The optical outputs of the LEDs were recorded using a UV/vis spectrophotometer (Lambda 650).

C. Thermal Conductivity Measurement

A thermal conductivity analyzer (Anter FLASHLINE 2000) was used to measure thermal conductivity using the flash light method. This involved uniform irradiation of a small disc-shaped specimen over its front face with a very short pulse of energy. The time–temperature history of the rear face was recorded through high-speed data acquisition with a solid-state optical sensor with very fast thermal response. Thermal diffusivity (mm^2/s) was determined from the time-dependent thermogram of the rear face. Thermal conductivity, κ, was automatically calculated as the product of thermal diffusivity, specific heat (J/gK), and density (g/cm^3). BN–epoxy nanocomposites containing various volume percentages of BN filler were cured and prepared in disc shape of 12.7 mm diameter and 0.3–3.0 mm thickness, depending on the actual thermal conductivity. The lower this value, the thinner is the sample required for a reliable value. For laminated BN-doped prepregs, the circular shape was prepared by using a Nd:YAG laser drilling system. The samples were ground flat on both sides, and coated with a silver layer on the bottom side and a graphite layer on the front surface. The former layer was used to enhance the thermal contact and prevent direct transmission of the flash light through the specimen, whereas the latter layer optimized the absorption of the flash light. Their weights and dimensions were measured with a balance and a vernier caliper, respectively. A standard copper block was used for calibration.

3. Thermal and Optical Modeling

To predict the thermal and optical performance of the LED package assembly, two commercial software packages are considered. For the thermal simulation models by Solidworks/Flow Simulation, the physical system is simplified by arranging multiple LEDs as the heat sources on a PCB surrounded by air. This software system solves the Navier–Stokes equations [29,30], which are the formulations of mass, momentum, and energy conservation laws of fluid flows. The equations in Ref. [31] are supplemented by fluid state equations defining the nature of the fluid and by empirical dependencies of fluid density, viscosity, and thermal conductivity on temperature. The numerical analysis is based on the first-order finite-difference method. The computational domain has the same size as the experimental models. It is discretized into equilateral triangular grids with a standard element size equal to 0.75 mm. The mesh height is finer than the width and length of the LED and PCB configurations. The convergence tolerance is set to be within 5% by the simulation software system. The initial and boundary conditions are shown in Table 1. As

Table 1. Material Data and Standard Boundary Conditions

Data and Boundary Conditions	Variable
Substrate material	Epoxy/MCPCB/FR4 PCB/PC
Material for solder pads	35 μm Cu (1 Oz)
Aluminum 5052 TC	150 W/m°C
Copper C1100 TC	385–400 W/m°C
Input current	0.1–2 A
Air velocity	Still air (free convection)
Heat transfer coefficient	25 W/m^2°C
Ambient temperature	25°C

for the optical models, the Solidworks/Tracepro simulation package is used, which can provide information such as light extraction efficiency, luminous efficiency, and color rendering index. The properties of the light sources of the LEDs were set in accordance with the specification provided by the suppliers, and the model was used for evaluating and predicting the illumination of the LEDs on the target plane with the candela distribution of the projected LED light sources. The model results of the thermal and optical performance of the LEDs were evaluated and compared with the experimental results.

4. Results and Discussion

Prior to the study of different environmental conditions for the LED array–PCB assembly, the effect of current change on the electroluminescence (EL) of the LED sample was first determined. A simple test configuration was used to measure the EL of the LED samples. Figures 2(a) and 2(b) show the EL spectra obtained from a Philips Lumileds LED sample with various currents passing through the LED sample mounted on a MCPCB. There are two emission bands in each curve: two blue emission peaks from the LED chip at 440 and 463 nm constitute the first band, and a yellow emission from the fluorescer centered at 517 nm is the second band. The spectral power distributions of the LED and the phosphor emission overlap: bipartition of the spectra was measured at a wavelength value $\lambda_{\text{cut}} = 488$ nm. With increasing current, the intensity of the yellow emission increases at nearly the same rate as the blue ones, which can be seen in the inset in Figs. 2(a) and 2(b). Linear increase of the 463 nm emission with current is observed. The positions of the peak wavelengths, 440 and 463 nm, are essentially the same (±0.2 nm) for all the EL spectra. The peak widths are also similar (full width at half maximum of ~50 nm) in the current range. The position of the yellow band does not change. The non-shifting blue emission peaks suggest that there is no band-filled effect [32].

To estimate the internal temperature of an operating LED, its surface temperature, as the case temperature, is considered and measured by using an IR camera and thermocouples. Case temperature is lower than the junction temperature of the LED

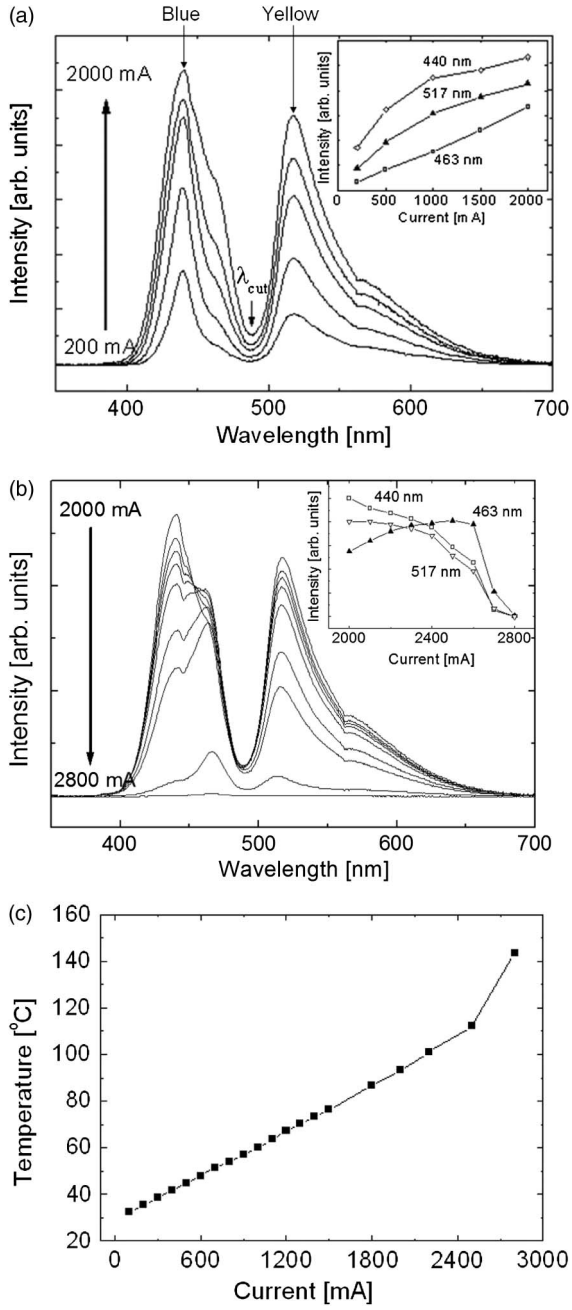

Fig. 2. Normalized electroluminescence (EL) spectra and case temperatures from a high-power white GaN/InGaN LED for the different currents indicated. The inset shows the amplitudes of the three emission peaks at various currents. (a) 200–2000 mA, (b) 2000–2800 mA, and (c) LED case temperature at different currents.

[33,34]. If the junction temperature increases, the case temperature will increase accordingly. Junction temperature can be obtained by the following equation [35]:

$$T_j = T_C + P\theta_{jc}, \tag{1}$$

where T_j = LED junction temperature, T_C = LED case temperature, P = drive power, and θ_{jc} is the

thermal resistance between the junction temperature and case temperature of the LED. Therefore, case temperature can be used as a parameter for estimating the LED lighting performance. The LED case temperatures for various currents were measured and plotted as in Fig. 2(c). The LED case temperature is directly proportional to the current. The result implies that an increase in LED case temperature will cause a shift in the color spectrum and a change in the lighting intensity. A better heat dissipation methodology from LED to PCB is therefore critical for maintaining a reliable optical performance.

A. BN–Epoxy Nanocomposites

The epoxy used in the study was a bisphenol-A phenolic resin with the brand name AFG-90. It was mixed with the hardener methylhexahydrophthalic anhydride (MHHPA) with structure in a ratio of 1:1.2 by weight, at room temperature. Epoxy based on this hardener improves thermal stability and peel strength. Different amounts of BN, used as the filler, were doped into the composite of the resin and the hardener (different weight ratios). They were then mixed by a magnetic stirrer for 2 h at a specific speed. Figure 3(a) shows the thermal simulation and experimental results. A typical LED is made of a die together with a lens as encapsulation and is then mounted on an epoxy substrate. As shown in the results, the thermal conductivity value increases from less than 0.5 W/mK to around 3 W/mK and can significantly decrease the junction temperature of a LED. Further increase in thermal conductivity will have a lesser impact on LED junction temperature suppression. The size distribution and scanning electron microscope (SEM) micrograph of the BN filler are shown in Fig. 3(b). It should be noted that the BN filler was platelet-shaped as observed from the typical SEM micrographs. The size distribution and SEM image of the BN filler for 15 μm are presented in the figure.

Theoretically, thermal resistance is caused by phonon scattering; thus, it has to be minimized to increase thermal conductivity. Materials with high thermal conductivities can be obtained by using fillers with high intrinsic conductivities. On the other hand, the aspect ratio of the filler is more worthy of consideration and it dictates the conductivities of a composite, because fillers with large aspect ratios easily form bridges between them, known as a conductive network. The formation of random bridges or networks from conductive particles facilitates electron and phonon transfer, leading to high conductivities. Figure 4 cannot be used to determine quantitatively the thermal conductive pathway and network; however, the SEM picture of the composite fracture surface reveals good interfacial adhesion between the BN filler and the epoxy matrix. The smooth interfaces between the filler and the resin is one of the significant contributions to the high thermal conductivity values of their composites as poor interfacial adhesion can lead to strong scattering of heat energy at the filler–matrix interfaces. It is easy to understand that more BN particles help to shorten the low thermal conductive path of the epoxy matrix and establish a high thermal conductive network for heat conduction. Therefore, a higher percentage of BN yields a higher thermal conductivity of the dielectric, which agrees with our experimental result. Comparing the SEM images of the variety of filler content in Fig. 4, improvement of thermal conductivity channels is significant when the BN

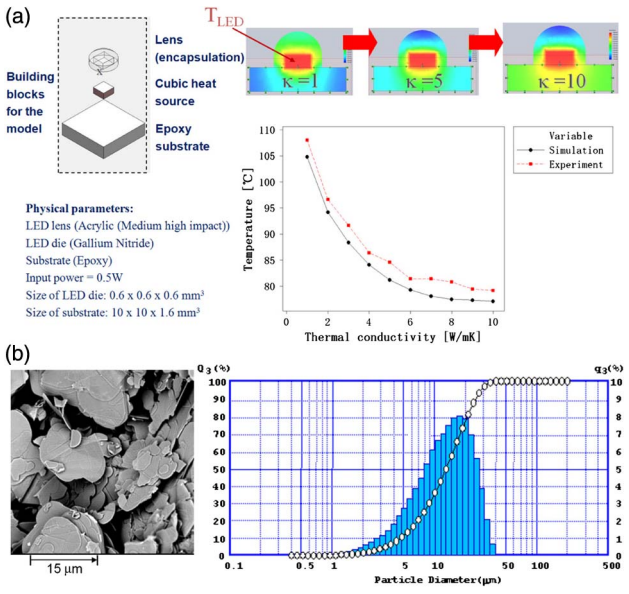

Fig. 3. Experimental and simulated thermal results for doped epoxy substrate. (a) Effect of substrate's thermal conductivity on LED junction temperature. (b) Size distribution and SEM micrograph of the BN filler for 15 μm.

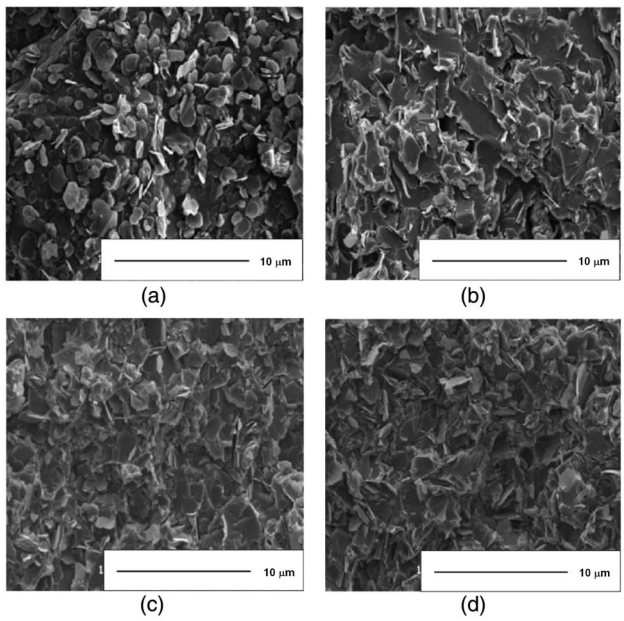

Fig. 4. SEM micrographs of BN-filled epoxy composite surfaces: (a) pure BN, (b) 10%, (c) 20%, and (d) 30%.

content increases from 0% to 20%. Beyond 20%, the difference is negligible when comparing 30% BN content with 20% content, in Figs. 4(c) and 4(d).

Identical high-brightness LEDs are selected and mounted on a pure epoxy and BN-doped nanocomposites having a particle size of 15 μm with 0, 20, and 30 wt. % content. The IR thermogram of the LEDs mounted on the BN–epoxy nanocomposites after BN content optimization is compared. All thermal images are at the same temperature scale. The LEDs are driven at 300 mA. In Fig. 5(a), the case temperature of the LED was 94.3°C, the highest among all three LEDs. BN–epoxy having a particle size of 15 μm with 30 wt. % could effectively lower the temperature by 21.5°C. It is strongly suggested that the effect of BN particle size on increasing thermal conductivity is significant for increasing the heat transfer between the crystal lattices. These BN particles result in a more effective way of improving thermal conductivity than other micron-sized particles and hence are more effective for lowering the LED case temperature.

Furthermore, the illuminance levels measured for the LEDs mounted on the BN-doped nanocomposites having a particle size of 15 μm with 0, 20, and 30 wt. % contents are 839, 932, and 956 lux, respectively.

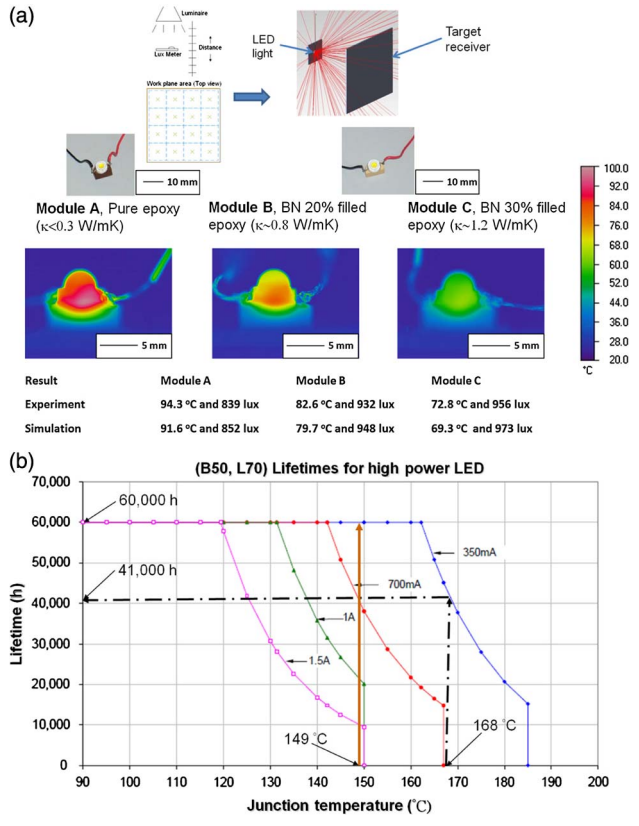

Fig. 5. (a) Experimental and simulated results of LED package for thermal and optical performance of different BN percentages in the BN–epoxy nanocomposite. (b) Reliability evaluation of the LED package on substrates in terms of lifetime analysis. The dotted arrow line is for the traditional FR4 substrate, whereas the solid arrow line is for the proposed BN–epoxy nanocomposite.

This indicates that the lighting power can be enhanced by increasing the percentage of the BN dopant in the composites.

As a reliability evaluation, the lifetime analysis of the LEDs placed on the conventional epoxy substrate and the proposed doped epoxy substrate is compared. For the conventional substrate, the measured LED case temperature was 143°C for a current of 0.35 A. Using Eq. (1) with a thermal resistance value of 25°C/W and a power value of 1 W, the calculated junction temperature is about 168°C. By fitting the value into the LED lifetime graph in Fig. 5(b), the lifetime is expected to be around 41,000 h. In this lifetime curve, the B50 value for the LED denotes the time by which 50% of the population is expected to fail and L70 is the time for the LED to maintain 70% lumen value. In comparison, for the LEDs placed on the substrate by the proposed doped method, a lower LED case temperature of ~124°C was measured for the same drive current. The junction temperature of the LEDs is calculated to be 149°C and the corresponding lifetime is found to be 60,000 h. In comparison, our proposed method to suppress the increase of LED case temperature would extend the LED lifetime by approximately 19,000 h over the conventional method. Accordingly, the reliability of the application of high-brightness LEDs would be improved significantly if the proposed doped epoxy substrate is used.

B. BN-Dielectric Layers of MCPCB

As shown in Fig. 6(a), a LED is mounted on a typical MCPCB. A dielectric layer is sandwiched between the LED and the metal plate. Five dielectric materials (Type A, Type B, Type C, Type D, and Type E) having different thermal conductivities were made

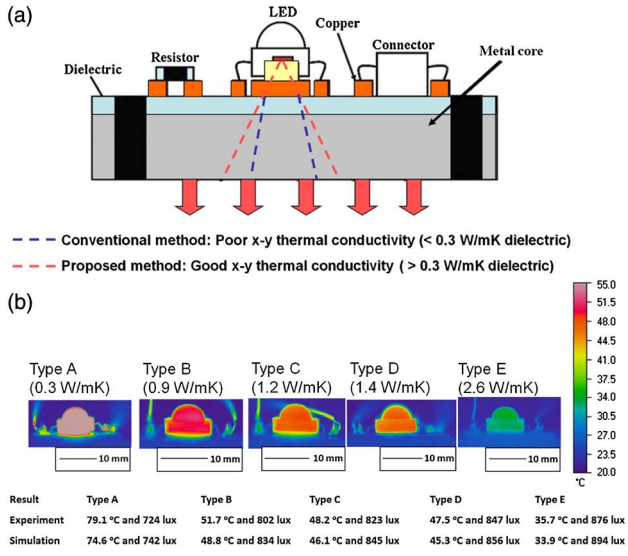

Fig. 6. Experimental setup and thermal and optical performance results for the LED MCPCB module. (a) Schematic diagram of a typical MCPCB and (b) experimental and simulated results of the LED package for dielectric layers with different thermal conductivities.

by blending BN with epoxy with percentages from 0% to 40% in weight, providing a flexible yet resilient coating on the base plate. An important characteristic of the dielectric layer is the amount of electrical isolation it provides between the copper on the topside and the metallic base plate on the underside. The thickness of the dielectric layer was 500 μm. A constant current of 0.4 A was supplied. Five identical LEDs were mounted on the five MCPCBs with different dielectric layers. The steady-state temperatures taken by the IR camera are shown in Fig. 6(b). The average case temperature of the LED mounted on the Type-A dielectric layer having a thermal conductivity of ~0.3 W/mK is about 79°C, whereas the temperature of the LED case on the Type-E dielectric layer having a thermal conductivity of ~2.6 W/mK drops to 35.7°C. In comparison, the heat accumulated feature appears in the thermal profile for the low-thermal conductivity dielectric layer, whereas the high-thermal conductivity dielectric layer does not exhibit this characteristic. A high-power LED mounted on a MCPCB with a dielectric layer having a higher thermal conductivity therefore dissipates thermal energy more efficiently through the PCB underneath (as the LED encapsulation material is of lower thermal conductivity). This allows heat to dissipate efficiently in all directions, as opposed to a slow-heat-dissipation MCPCB with a dielectric layer having a lower thermal conductivity. It should be noted that the voltage drops across the LEDs on the MCPCBs (dielectric materials with high thermal conductivity and low thermal conductivity) are 3.245 and 3.1935 V, respectively, at the constant current mode. As LED power is governed by voltage and current, the illuminance level output of the LEDs on these two types of MCPCBs will therefore be different for a given constant current. This also shows that good heat dissipation from the LED to the MCPCB with a better dielectric layer could help to improve the optical performance.

In accordance with Fourier law, steady-state uniform heat conduction through a thin sample can be expressed as follows:

$$\frac{q}{A} = -\kappa \frac{dT}{dx}, \tag{2}$$

where q = heat flow rate (W), A = area of sample (m^2), κ = thermal conductivity (W/mK), x = thickness of specimen (m), and dT/dx = temperature gradient through the sample (K/m).

The thermal resistance of the dielectric sample (R) can be expressed as $R = ((\Delta T)/(q/A))$ and $R = (\Delta x/\kappa)$. It is clear that resistance is proportional to the ratio of the material thickness to the material thermal conductivity. As the test structures of these kinds of MCPCB were exactly the same, except in the dielectric layer region, the heat transfer mechanisms in the regions between the LED chip and the MCPCB were very similar but showed different behavior within the MCPCB dielectric region. The thermal resistance of the dielectric layer varies due to a difference in the thermal conductivity in the test condition. These results show better performance for a MCPCB having the highest thermal conductivity, which means that the junction temperature can be lowered, giving the LEDs a longer lifetime.

C. BN-Doped FR4

The prepared BN–epoxy nanocomposite was reinforced with E-Glass fiber cloth 7628 (plain, 0.2 mm, 200 g/m^2) to form a prepreg layer. E-Glass fiber 7628 was coated with the prepared nanocomposite. It was then put into an oven set at 60°C for 4 h for pre-curing. For fabricating the PCB as shown in Fig. 7(a), eight pieces of prepregs were placed on top of each other and pressed by a pressing machine to laminate them with copper foil on both sides, forming the BN-filled FR4.

Eight layers of 7628 prepregs were used for laminating one sheet of 1.2 mm FR4. The laminated boards were then cut to square shape of length 30 mm. The BN-filled laminated board having the highest thermal conductivity, of 0.65 W/mK was selected. Figure 7(b) shows a photo of the FR4 and the laminated board having a LED mounted on top, and also displays the corresponding thermal images. The thermal image clearly shows that the

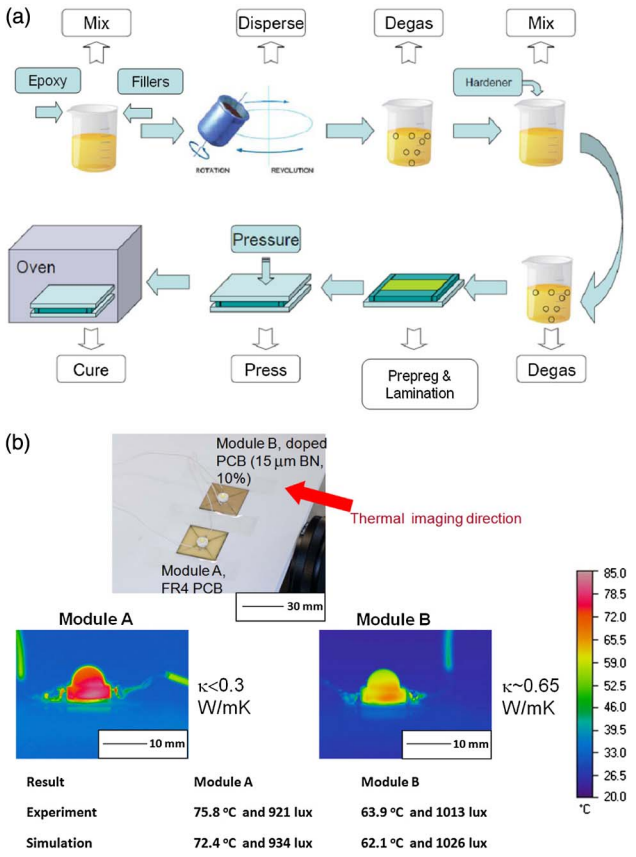

Fig. 7. (a) Lamination workflow for the BN-doped PCB. (b) Thermal and optical performance results of the LED package mounted on the conventional FR4 PCB and the BN-doped PCB.

BN-filled laminated PCB can effectively lower the LED case temperature from 75.8°C to 63.9°C. This is a 15.7% decrease in LED case temperature. LED luminance was measured with a lux meter and was found to be 921 and 1013 lux for the LED mounted on the FR4 PCB ($\kappa < 0.3$ W/mK) and the BN-filled PCB ($\kappa = 0.65$ W/mK), respectively. This is a 9.9% increase in lighting power. Generally, when LEDs are lit continuously, an accumulation of heat is concentrated in the LED die if a traditional FR4 substrate is used. By adding high-thermal conductivity filler into the substrate material, its heat dissipation process can be enhanced. The last issue would be the additional material cost as to whether it can make the overall substrate price competitive.

D. BN-Doped PC

As shown in Fig. 8(a), a LED package was mounted on a commercial PC material blended with BN filler with different thermal conductivities. The filling percentages varied from 0% to 30% in weight. A constant current of 0.3 A was supplied. The steady-state temperatures taken by the IR camera are shown in Fig. 8(a). The average case temperature of the LED mounted on module A having a thermal conductivity of ~0.18 W/mK is about 64.4°C, whereas the temperature of the LED case on module D having a thermal conductivity of ~0.45 W/mK drops to 58.7°C. There is about 8.9% suppression in LED case temperature when the thermoplastic material is filled with BN.One potential application of this filler mixing is on the enclosure cover of a commercial LED light bulb, shown in Fig. 8(b). In this work, two kinds of enclosure cover were molded. One was pure PC whereas the other was PC filled with BN. A commercial 3 W LED light bulb was used for the IR imaging experiment as shown in Figs. 8(b) and 8(c). Thermal images, with and without enclosure, were taken. As marked in Fig. 8(b), there are 10 points along the dashed line in the front LED view. The measured temperatures of the points are shown in the figure. Points 1–3 are around the surroundings of the LED light bulb. Points 4–6 are close to the edge of the heat sink. Point 7 is at the edge of the PCB. Points 8–10 are on the surface of the PCB on which the LEDs are mounted. By comparison, Point 8 has a higher temperature than Point 10. This is attributed to the higher heat accumulation in the region closer to the LED. In Fig. 8(c)(i), it can be observed from the thermal plot that there was an accumulation of heat in the enclosure at the top region, which is potentially damaging to the LED package assembly. Overheating can shorten the life expectancy of the LED system or lead to catastrophic failure. Chimney effect pressures around the LEDs inside the enclosure are generated by differences in air density due to temperature, i.e., hot air rises and cold air sinks. This effect due to LED heat sources within a local exhaust enclosure produces convective air currents with vertical velocities proportional to the rate of heat transferred to the surrounding air and to the height of the rise of the heated air. When hot gases rise through an enclosure, the vertical stack exit velocity is proportional to the square root of the difference in density between the heated air column and an equal column of the surrounding ambient air. This can cause further heat accumulation in the LED surroundings if high-power LEDs are used. The temperature measured at points 5, 6, 7, 8, 9, and 10 at the enclosure surface of the light bulb without BN doping is about 3°C is higher than that of the enclosure with BN doping in Fig. 8(c)(ii). By comparison, the thermal distribution for the enclosure surface with BN doping was more uniform and heat was dissipated better. An enclosure material with higher thermal conductivity is suggested to be used to avoid hot air being trapped in the light bulb enclosure. As less heat was trapped in the enclosure material with BN doping than in the enclosure without BN, the measured illuminance level increased from 636

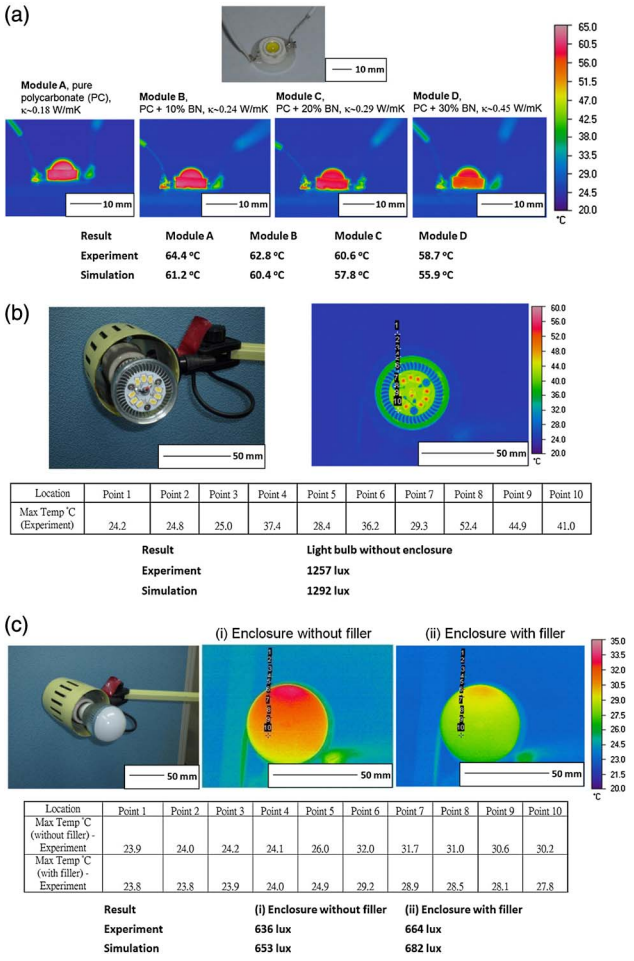

Fig. 8. Experimental and simulated results for the doped PC enclosure of an LED light bulb in terms of thermal and optical performance. (a) IR thermograms for LED package mounted on different BN-filled PC substrates. (b) LED light bulb without enclosure. (c) LED light bulb with enclosure [(i), enclosure without filler; (ii), enclosure with filler].

to 664 lux, i.e., 4.4% improvement in optical performance.

In this work, there is about a 5% discrepancy between the thermal simulated and experimental results. The cause is suggested as being the change of environmental conditions and variance of the LED die quality. When the optically simulated and experimental results are compared, discrepancy is about 10%. The cause of the higher discrepancy is suggested to be the excessive heat generation from the chips in the LED package, which reduces the optical behavior due to various factors, such as material degradation, contamination, and de-laminations in the LED chips. As a constant current mode of the LEDs was used in the test, the change in voltage under different conditions indicated a simultaneous change in power consumption. The above results demonstrate the use of BN filler on LED package assembly by converting the minimum electrical energy wastage into heat for benchmarking the energy saving throughout the product life cycle.

5. Conclusions

In this study, thermally conductive BN-filled nanocomposites were prepared successfully. The issues of thermal management and optical performance of a LED package assembly were addressed using these BN fillers. The effects of the thermal conductivity of the substrates on the temperature distribution of the LED package assembly were analyzed systematically and optimized for producing higher lighting efficacy and efficient heat dissipation. Using the proposed approach, significant improvement in heat dissipation was observed from the LED to the substrate and the surrounding. In addition, the thermal model developed facilitates electronic design with minimum possible power dissipation and clarifies the heat transfer mechanism in the LED package assembly. The proposed polymer composite has been demonstrated as being important for effective thermal management of high-power LED packages on substrates.

This work was funded by the Guangdong Provincial Department of Science and Technology under the Scheme of Emerging Strategic Industry (project number 2012A080304007).

References

1. N. Narendran and Y. M. Gu, "Life of LED-based white light sources," J. Disp. Technol. **1**, 167–171 (2005).
2. J. Zhou and W. Yan, "Experimental investigation on the performance characteristics of white LEDs used in illumination application," in *Proceedings of the 38th IEEE Power Electronics Specialists Conference (PESC'07)*, Orlando, Florida, 2007, pp. 1436–1440.
3. K. W. Garrett and H. M. Rosenberg, "The thermal conductivity of epoxy-resin/powder composite materials," J. Phys. D **7**, 1247–1258 (1974).
4. H. J. Ott, "Thermal conductivity of composite materials," J. Plast. Rubber Process. Appl. **1**, 9–24 (1981).
5. P. Procter and J. Solc, "Improved thermal conductivity in microelectronic encapsulants," IEEE Trans. Compon., Hybrids, Manuf. Technol. **14**, 708–713 (1991).
6. H. He, R. Fu, Y. Han, Y. Shen, and X. Song, "Thermal conductivity of ceramic particle filled polymer composites and theoretical predictions," J. Mater. Sci. **42**, 6749–6754 (2007).
7. D. M. Bigg, "Thermally conductive polymer compositions," Polym. Compos. **7**, 125–140 (1986).
8. D. P. H. Hasselman and L. D. Johnson, "Effective thermal conductivity of composites with interfacial thermal barrier resistance," J. Compos. Mater. **21**, 508–515 (1987).
9. Z. Li, K. Okamoto, Y. Ohki, and T. Tanaka, "Effects of nano-filler addition on partial discharge resistance and dielectric breakdown strength of Micro-Al_2O_3 Epoxy composite," IEEE Trans. Dielectr. Electr. Insul. **17**, 653–661 (2010).
10. MCPCB Applications. Available: http://www.cofan-pcb.com/products/mcpcb.php.
11. H. M. Cho and H. J. Kim, "Metal-core printed circuit board with alumina layer by aerosol deposition process," IEEE Electron Device Lett. **29**, 991–993 (2008).
12. R. R. Tummala, E. J. Rymaszewski, and A. G. Klopfenstein, *Microelectronics Packaging Handbook: Subsystem Packaging*, 3rd ed. (Kluwer Academic, 2001), Part 3, pp. 85–86.
13. C. I. Nicholls and H. M. Rosenberg, "The excitation spectrum of epoxy resins; neutron diffraction, specific heat and thermal conductivity at low temperatures," J. Phys. C **17**, 1165–1178 (1984).
14. A. A. Solomo, J. Fourcade, S. G. Lee, S. K. Kuchibhotla, S. Revankar, P. L. Holman, and J. K. McCoy, "The polymer impregnation and pyrolysis method for producing enhanced conductivity LWR fuels," in *Proceedings of the 2004 International Meeting on LWR Fuel Performance*, Orlando, Florida, 2004, pp. 146–155.
15. J. K. Kim, J. W. Kim, M. I. Kim, and M. S. Song, "Thermal conductivity and adhesion properties of thermally conductive pressure-sensitive adhesives," Macromol. Res. **14**, 517–523 (2006).
16. M. Hussain, Y. Oku, A. Nakahira, and K. Niihara, "Effects of wet ball-milling on particle dispersion and mechanical properties of particulate epoxy composites," Mater. Lett. **26**, 177–184 (1996).
17. P. Bujard, G. Kühlein, S. Ino, and T. Shiobara, "Thermal conductivity of molding compounds for plastic packaging," IEEE Trans. Compon., Packag., Manuf. Technol., Part A **17**, 527–532 (1994).
18. Y. S. Xu, D. D. L. Chung, and C. Mroz, "Thermally conducting aluminum nitride polymer-matrix composites," Composites, Part A **32**, 1749–1757 (2001).
19. W. Kim, J. W. Bae, I. D. Choi, and Y. S. Kim, "Thermally conductive EMD (Epoxy Molding Compound) for microelectronic encapsulation," Polym. Eng. Sci. **39**, 756–766 (1999).
20. W. Bae, W. Kim, S. W. Park, C. S. Ha, and J. K. Lee, "Advanced underfill for high thermal reliability," J. Appl. Polym. Sci. **83**, 2617–2624 (2002).
21. M. T. Huang and H. Ishida, "Investigation of the boron nitride/polybenzoxazine interphase," J. Polym. Sci. B **37**, 2360–2372 (1999).
22. R. S. Pease, "An x-ray study of boron nitride," Acta Crystallogr. **5**, 356–361 (1952).
23. C. J. Weng, "Advanced thermal enhancement and management of LED packages," Int. Commun. Heat Mass Transfer **36**, 245–248 (2009).
24. B. M. Song, B. Han, A. Bar-Cohen, R. Sharma, and M. Arik, "Hierarchical life prediction model for actively cooled LED based luminaire," IEEE Trans. Compon., Packag. Technol., Part A **33**, 728–737 (2010).
25. M. H. Chang, D. Das, P. Varde, and M. Pecht, "Light emitting diodes reliability review," Microelectron. Reliab. **52**, 762–782 (2012).
26. C. T. Yang, W. C. Liu, and C. Y. Liu, "Measurement of thermal resistance of first-level Cu substrate used in high-power multi-chips LED package," Microelectron. Reliab. **52**, 855–860 (2012).
27. B. Witzen, "LED thermal design challenges: tips and techniques," ECN Magazine, August 2010.
28. MuAnalysis Inc., "Lumileds Luxeon K2 LED lamp teardown and technology analysis," 2008. Available: http://www.muanalysis.com/_documents/publications/Teardown%20reports/

Lumileds-Luxeon-K2-LED-Lamp-Teardown-Report-short-version.pdf.
29. D. J. Acheson, *Elementary Fluid Dynamics*, Oxford Applied Mathematics and Computing Science Series (Oxford University, 1990), pp. 30–32.
30. T. E. Faber, *Fluid Dynamics for Physicists* (Cambridge University, 1995), pp. 204–244.
31. Solidworks Flow Simulation Technical Reference, 2009.
32. T. N. Morgan, "Broadening of impurity bands in heavily doped semiconductors," Phys. Rev. **139**, A343–A348 (1965).
33. M. Ford, "In-situ LED junction temperature and thermal resistance," Vektrex Application Note, 2008. Available: http://www.vektrex.com.
34. J. Hulett and C. Kelly, "Measuring LED junction temperature," Photon. Spect. 2008. Available: http://www.photonics.com/Article.aspx?AID=34316.
35. W. J. Hwang, T. H. Lee, L. Kim, and M. W. Shin, "Determination of junction temperature and thermal resistance in the GaN-based LEDs using direct temperature measurement," Phys. Status Solidi C **1**, 2429–2432 (2004).